ABSTRACT

Methods of Determining Stream Setback Corridors in Urban Watersheds from Remotely Sensed Data in the Dallas Metropolitan Area, Texas

Matthew R. Schreiner, M.A.

Mentor: Peter M. Allen, Ph.D.

Bank stability in urbanized streams is worsening in response to increased runoff, causing unprecedented stream erosion. Eroding banks pose a serious threat to existing structures prompting cities to create buffer zone ordinances to prevent the loss of future structures. Unfortunately, most ordinances probably misjudge buffer zone widths due to the lack of sufficient topographic accuracy for their delineation. However, this study utilizes observations based from remotely sensed data, such as Light Detection and Ranging (LiDAR) with higher accuracy, as well as geological parameters such as channel material.

Stream setbacks are easily calculated using computer-aided mapping technology, through the use of remotely sensed data and setbacks can be determined and mapped as corridors with minimal field checking. This study evaluates the overall accuracy of this methodology as compared with values acquired in the field. The results show that the LiDAR data, while being a relatively good fit to the field data, can misrepresent stream setbacks in areas of high relief, most likely due to the smoothing algorithms used in the post-processing of the raw LiDAR data, and field checking is advocated.

Methods of Determining Stream Setback Corridors in Urban Watersheds from Remotely Sensed Data in the Dallas Metropolitan Area, Texas

by

Matthew R. Schreiner, B.A.

A Thesis

Approved by the Department of Geology

____
Steven G. Driese, Ph.D., Chairperson

Submitted to the Graduate Faculty of
Baylor University in Partial Fulfillment of the
Requirements for the Degree
of
Master of Arts

Approved by the Thesis Committee

____
Peter M. Allen, Ph.D., Chairperson

____
Vincent S. Cronin, Ph.D.

____
Joseph D. White, Ph.D.

Accepted by the Graduate School
December 2009

____
J. Larry Lyon, Ph.D., Dean

Page bearing signatures is kept on file in the Graduate School.

TABLE OF CONTENTS

LIST OF FIGURES

LIST OF TABLES

ACKNOWLEDGMENTS

I would like to thank Dr. Peter Allen for all the time and effort put into reading and re-reading this document as it went through its various stages of development. I would also like to thank him for the opportunity to study with him throughout my semesters here at Baylor. I would like to thank Dr. Vincent Cronin and Dr. Joseph White for reviewing and offering their input to this work as well. I would also like to extend my gratitude to Dr. Shane Prochnow who assisted me with getting this project off the ground and Bruce Byars for helping me with everything that's come up in the past year, including being my eyes and ears around the department when life took me elsewhere. Special thanks go out to my father, Rick Schreiner, who helped me with the field collection of my data, and my wife, Tina, for always finding the words to keep me going. And to the rest of my extended family, thank you for your words of encouragement and continued interest into my field of study.

CHAPTER ONE

Introduction

The effect of urbanization on natural stream channels is of concern to both regulatory agencies and developers. Urbanization has led to a variety of problems including increased channel erosion and flooding. Land that was once used for agriculture or pasture has been converted to roads, parking lots, buildings, gardens and lawns. Rainfall that, in a natural environment, infiltrates the soil and is released gradually into streams and creeks as baseflow, is quickly drained in an urban environment, to streams and creeks via storm sewers, increasing peak flows (Doyle, et al., 2000; Finkenbine, et al., 2000).

While peak discharge is increased at all recurrence intervals, the most profound increases are seen at the two year and five year flood recurrence intervals, which affects channel erosion. Both Land and others (1982) and Dempster (1974) have observed 81% and 80% increases in five-year flood-recurrence peak flows, respectively, in the Dallas/Fort Worth area. Veenhuis and Gannett (1986) also observed increases; 99% in two year floods and 82% in five year floods in the Austin area.

With the increase in urban peak flows, smaller urbanized streams begin to undergo changes. Channels can widen by a factor of 2 to 3 and downcut between 2 to 6.1 meters (6.5 to 20 feet) (Chin, 2006; Simon and Hupp, 1986; Thorne, 1999). Such increases in discharge and related incision cause steepening of slopes, slope failures, widening and aggregation (Schumm, 1999). This process is illustrated by the Simon and Hupp (1986) Channel Evolution Model (CEM), which shows how urban channels adjust by first downcutting, then widening, and finally establishing a new floodplain (Fig 1.)

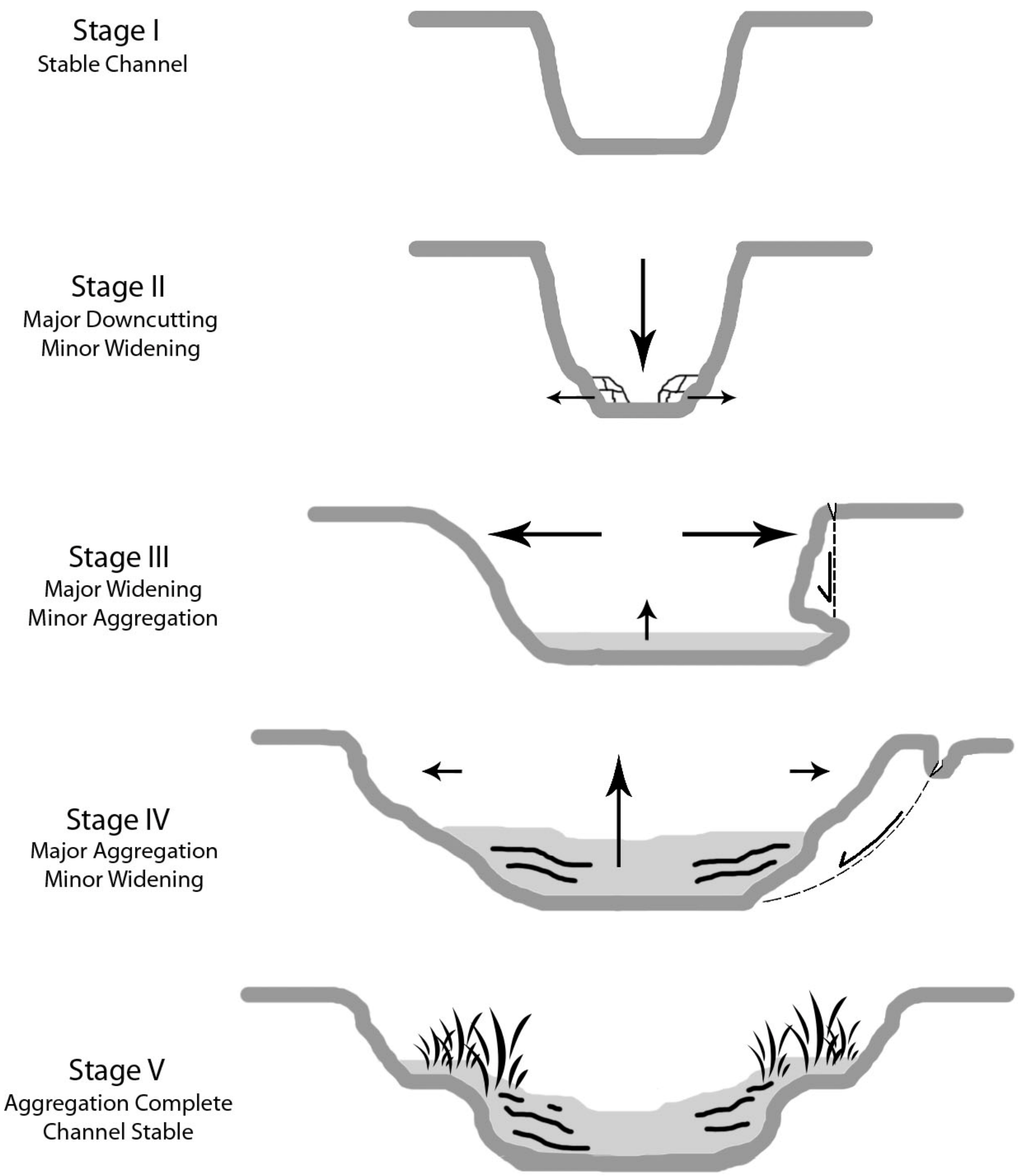

Figure 1. The Simon and Hupp (1986) Channel Evolution Model (Adapted from Ayres Associates, 2004) Channels of particular interest in this study are those in Stage II or in Stage III.

Incising and widening channels pose a serious threat to existing structures, such as bridges, houses and other infrastructure. Attempts to solve this problem are expensive and average $50 a square foot-- up to $25,000 to $300,000 for one lot (Allen, 2009). In addition, streambank erosion and related sedimentation impacts local biology, making conditions less habitable for riparian buffer zone vegetation and creek-dwelling species (Finkenbine, 2000). The loss of bank vegetation can also have a detrimental impact on bank stability; channels that lose their riparian buffer zone due to incision experience a dramatic decrease in friction angle (Φ`), a major indicator of stability (Millar, 2000).

Preventative Measures

In the past, the primary method utilized to prevent development in hazardous areas near stream channels was through building codes that reference 100-year floodplain zonation maps, such as the ones published by the National Flood Insurance Program (NFIP; Ayres Assoicates, 2004). While this criterion has proven beneficial in preventing structural loss along larger channels due to flooding, it has not prevented homes being built near the stream in smaller channels where the 100-year flood boundaries are often within the banks of incised channels (Fig. 2). The result is development along these smaller systems where the stream banks are outside the 100-year flood zone, but within the zone in which stream-channel depth and width are changing due to the increase in runoff.

There are two potential solutions to solving stream bank erosion and slope stability problems in smaller streams. For areas that have already been urbanized and are now subject to the effects of channel incision and widening, the solution relies on costly engineering designs such as gabions or drop structures that can provide local protection

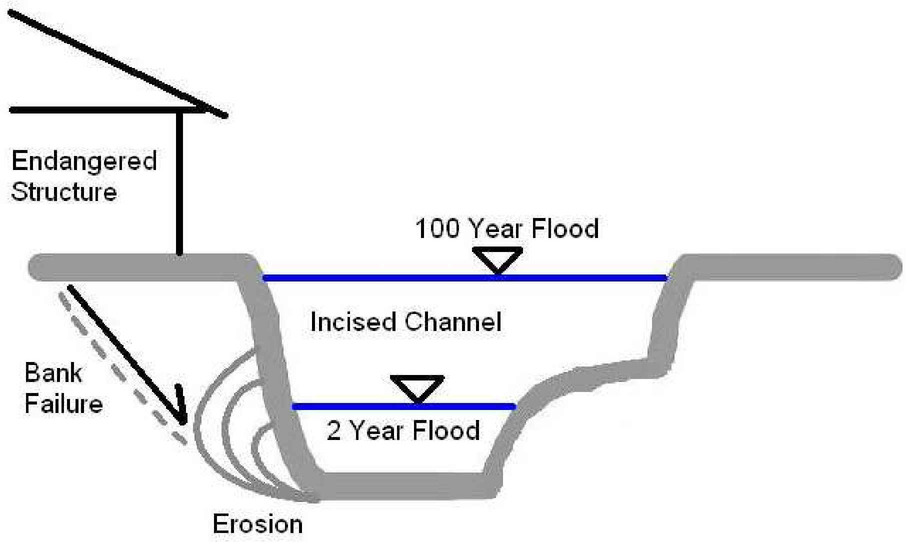

Figure 2. In smaller streams, the 100 year floodplain may not extend beyond the channel, especially if the channel is incised. This does not negate the danger of building near the channel, however.

to structures (Schumm, 1999). These engineering techniques will also have a profound impact on local habitat as well as erosion rates in other parts of the stream. The second solution involves preventative techniques which incorporate use of setbacks that can be implemented prior to urbanization.

Setbacks are directly related to stream processes, bed and bank materials and differences in topography. Instead of relying on a pre-determined distance from the stream as buffers, distances are determined by using an angular ratio, as 4 to 1 to 6.5 to 1, measured from the toe of the bank. Setbacks are based on the bank material and erosion potential of the stream (Cruden et al., 1989). These methodologies have been incorporated with setback ordinances for the city of Dallas and Austin (City of Dallas, 1991; Ayres Associates, 2004).

While ordinances are enforced for specific building sites, it would be advantageous for cities to have maps indicating the geographic extent of such no build zones. This would allow the developer to assess developable land and allow cities to more efficiently regulate development. With the advent of more detailed topographic data (Light Detection and Ranging, LiDAR) and Geographic Information Systems (GIS) technologies, it should be possible to determine setbacks and draw them on maps. The purpose of this resource is to (1) test the mechanics of applying setbacks using GIS methodologies and (2) the accuracy of such setbacks compared to field measurements.

For this project, a setback algorithm will be produced from various hydrologic equations that will allow users to input stream bank parameters typically surveyed in the field in order to calculate a setback length. The algorithm, which is capable of calculating multiple cross sections worth of data at once, will be used to create a corridor of setbacks along several stream segments. Once this benchmark is established, bank parameters from remotely sensed datasets will be fed into this algorithm to create additional setbacks on the same stream segments in order to determine if these data serve as an appropriate substitute for the field survey. Finally, the significance of the remotely sensed data will be analyzed, and implications of the field data will be discussed.

Study Area

The study area is within the central Texas ecoregions known as the Blackland Prairie and Cross Timbers (Fig. 3), a large north-south belt of agriculturally productive land with and area of 17,000 square miles (Harmel, et al., 2006). Population in these regions have exploded since the 1960s (Fig. 4, 5), and is expected to double over the next 50 years (TCEQ, 2006). The major metropolitan areas of Dallas/Forth Worth, Austin and

Figure 3. The location of the Blackland Prairie and Cross Timbers in Texas (adapted from Texas Parks and Wildlife, 1978). Three major cities as well as numerous smaller towns such as Waco, Hillsboro and San Marcos, make this area one of the major population belts of Texas.

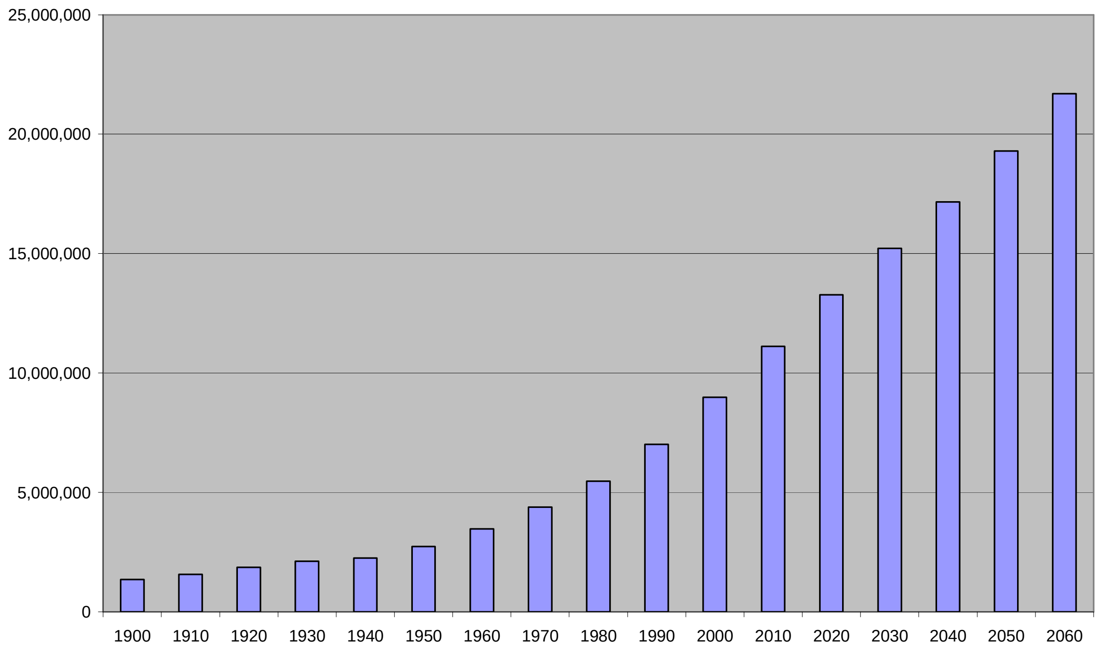

Figure 4. Historical and projected estimate of population living within the Blackland Prairie (Texas Water Development Board, 2006)

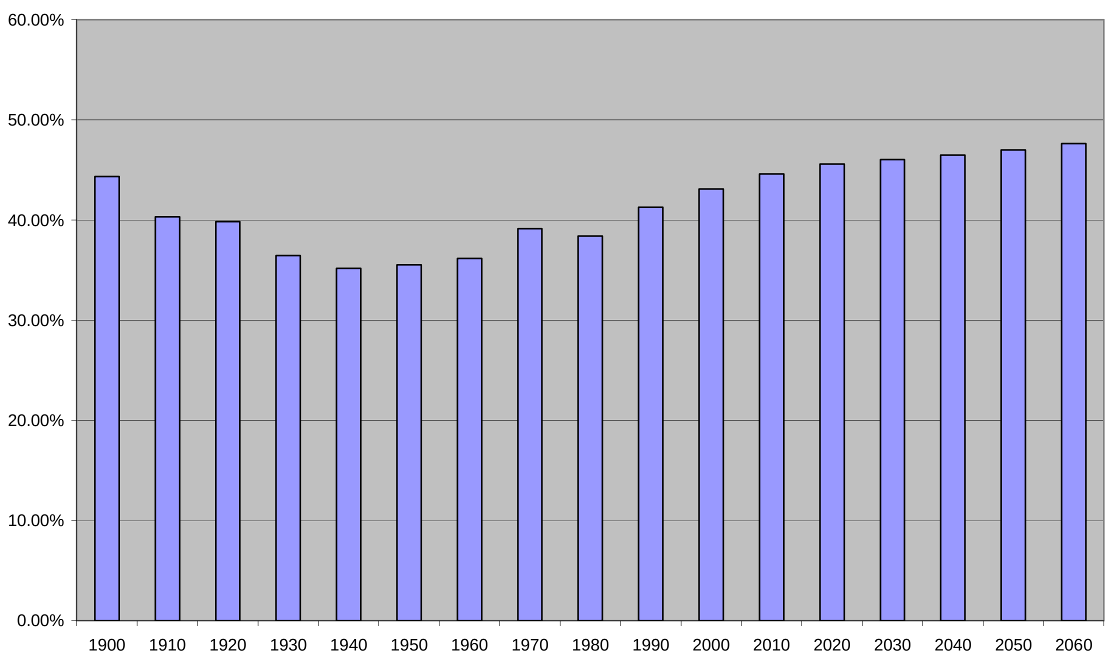

Figure 5. Historical and projected estimates of the percentage of all Texans who have or will live in the Blackland Prairie (Texas Water Development Board, 2006).

San Antonio all lie within these two physiographic prairies, which contains approximately 45% of the state population.

The Blackland Prairies are known for extensive runoff and soil loss (Allen, 1975; Baldwin, 1974). The northernmost portion of this region is the most affected by these processes, having the greatest average annual rainfall and runoff estimates (Figs. 6, 7). Studies on erosion in this area have shown annual channel erosion rates between 23 and 572 mm (Capello, 2008). Channel enlargement with urbanization in these shale and

Average Annual Precipitation, Inches

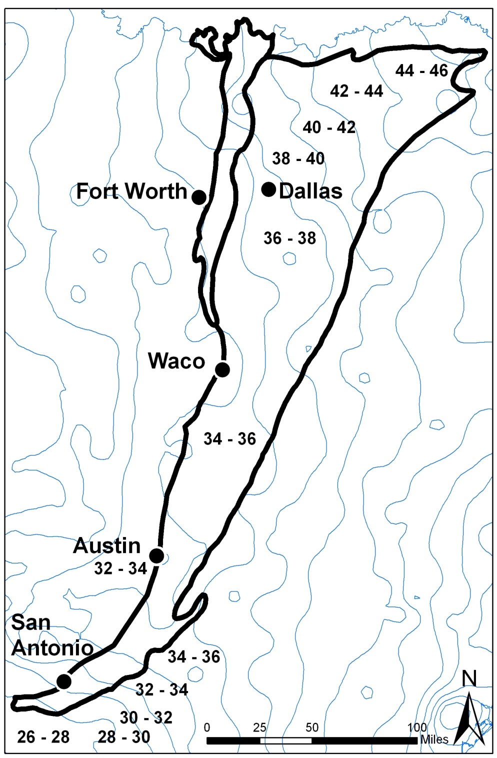

Figure 6. Average annual rainfall estimates, in inches, for the study area (adapted from Daly and Taylor, 1998). The greatest amounts of annual precipitation occur in the northern areas, where the study area is located.

Average Annual Runoff, Inches

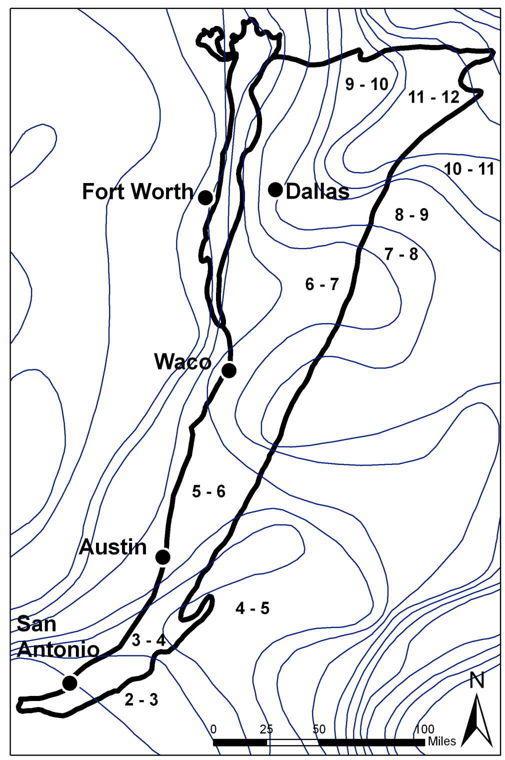

Figure 7. Average annual runoff estimates, in inches, for the study area (adapted from Gebert, et al., 1987). Note that the greatest amount of runoff occurs in the northern regions, where the study areas are located.

limestone formations can range from 1.7 to 2.4 times as large in both width and depth (Allen and Narramore, 1985). Similarly, in the Woodbine Formation, channels in urbanized watersheds are 1.17 to 2.11 times wider and 1.03 to 1.45 times deeper than natural channels (Robinson, 1982). Low shear strengths, low unconfined compressive strengths and low slope stability make these formations extremely susceptible to bank failure following erosion that steepens stream banks (Font and Williamson, 1970; Garner and Young, 1976; Robinson, 1982). Table 1 details the engineering properties of the pertinent formations to this study. For example, the Ozan Formation's unconfined compressive strength ranges from 12.5 to 347 pounds per square inch, the shear strength averages 29.15 pounds per square inch, the swell potential is 19.9 pounds per square inch, the material becomes unstable at 10° to 20° and is prone to several types of failures, and has a plasticity index between 35 and 49. The material's strength and slope stability reveal which formations are prone to erosion and slope failures. Eagle Ford Shale (Fig.

Table 1. Engineering properties of the pertinent geological formations. (Font and Williamson, 1970; Garner and Young, 1976; Narramore and Allen, 1985; The Earth Technology Corporation, 1990; Hsu and Nelson, 2002)

Formation	Unconfined Compressive Strength	Shear Strength	Swell Potential	Slope Stability	Plasticity Index
Ozan (Taylor Marl)	12.5 - 347 PSI	29.15 PSI	19.9 PSI	10°- 20°, prone to slumps, infinite and wedge failures	35 - 49
Austin Chalk	347 - 3472 PSI	109.5 PSI	Low	> 45°, prone to planar failures	26 - 34
Eagle Ford Shale	12.5 - 347 PSI	10 - 50 PSI	35.8 PSI	0° - 20°, prone to slumps, infinite and wedge failures	34 - 48
Woodbine Sand	1.39 - 97.2 PSI	Low	Low	Low, prone to slumps and infinite failure	4 - 40

8) has some of the lowest shearing and compressive strengths and is prone to several types of slope failures. The Woodbine Formation (Fig. 9) is similarly susceptible to failure. The Austin Chalk (Fig. 10) is the most resilient of the group, with the highest

Figure 8. Grapevine Creek, which is located in the Eagle Ford shale. The fracturing and low shear strength cause the shale to be easily eroded in flood events.

Figure 9. Timber Creek, an alluvial channel in the Woodbine Formation, which is very susceptible to erosion.

Figure 10. Duck Creek, which has eroded to the Austin Chalk. The greater strength parameters make it harder to erode.

strength parameters. Slope failure in this formation usually only occurs when the formation is undercut along faults and joint planes. Figure 11 shows how these formations fall stratigraphically in Dallas County.

Study Sites

The study area is focused on three watersheds in the Dallas/Fort Worth metroplex. The watersheds were selected based on the following criteria: (1) Each watershed must be located predominately within one representative geologic formation (sandstone, shale, marl or limestone), (2) each watershed must be actively eroding; in phase 2 (downcutting) or phase 3 (widening) of the Channel Evolution Model (CEM, Simon and Hupp, 1986) (Fig. 1), (3) each watershed should be between 10 and 20 square miles in order to keep the runoff values roughly similar.

From these criterions, three watersheds were selected for analysis. Grapevine Creek in Coppell, Texas, Timber Creek, in Lewisville, Texas, and Duck Creek, in Garland, Texas. Figure 12 shows the relative location of all three watersheds around the Dallas/Fort Worth Metroplex, while figure 13 illustrates the watershed geology.

Based on available data on urban channel widths in the north central Texas area compiled by Narramore (1981), the channel top widths for streams in this area average 100 feet. Based on criteria for reference reaches set forth by Rosgen (1998), a 2000 foot segment (20 channel widths) was isolated for analysis. The reaches selected were located in urbanized residential areas on 1^{st} and 2^{nd} order streams, which account for between 70 and 77 percent of drainage in this area (Allen, 1977; Leopold, et al. 1964).

The representative reach isolated for Grapevine Creek is a shale bedrock channel completely contained within outcropping Eagle Ford Shale Formation in the Silawa soil

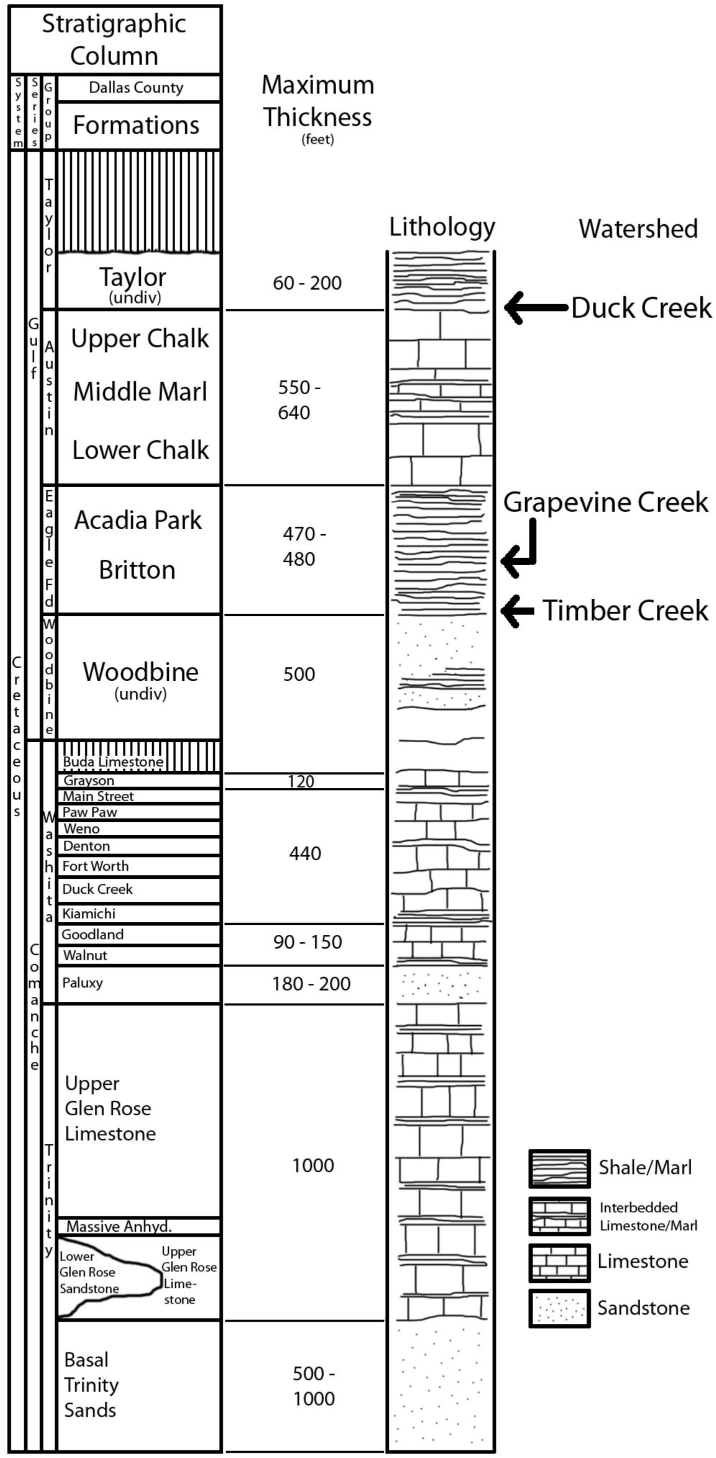

Figure 11. Stratigraphic column of the geology in Dallas county (adapted from Allen et al, 1993). Also indicated are where the three watersheds are located on the column.

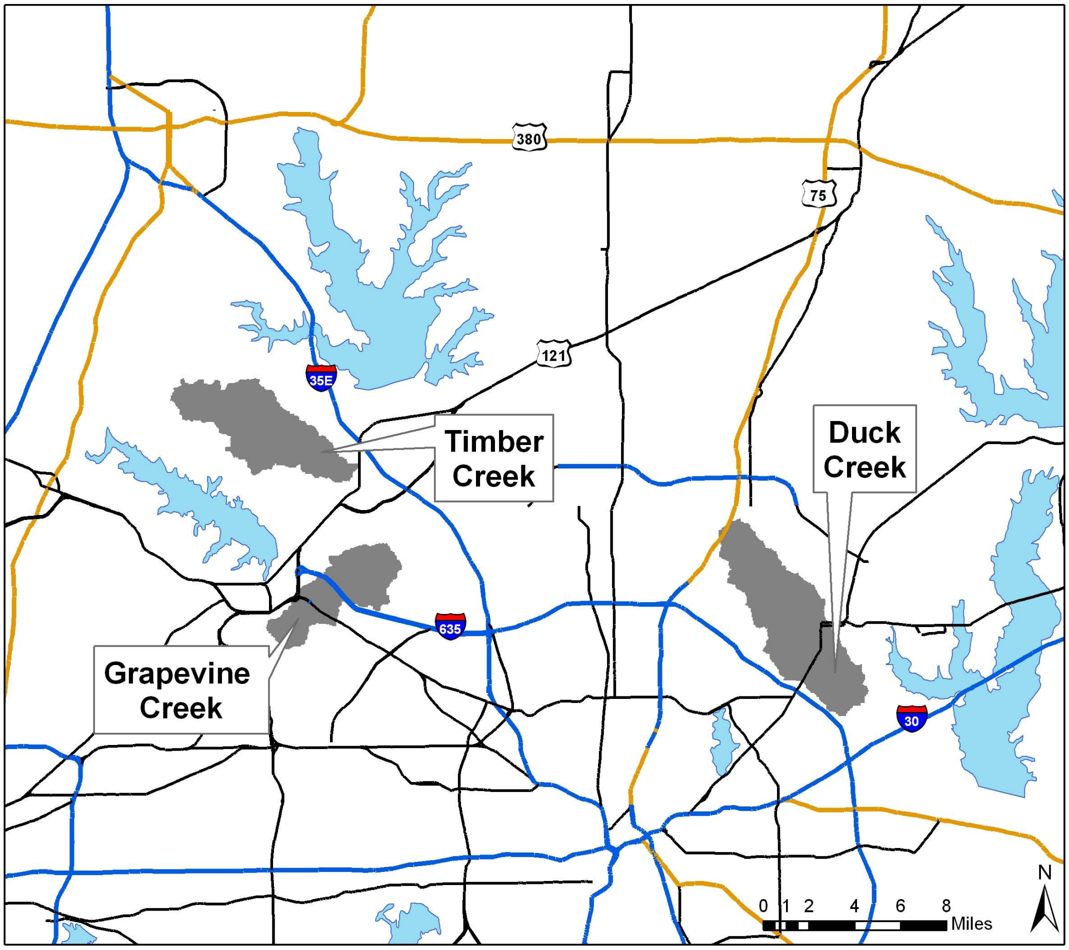

Figure 12. The relative location of the three watersheds used in the study. All three are located in heavily populated suburbs of Dallas. Grapevine Creek is located in Coppell, Timber Creek is located in Lewisville, and Duck Creek is located in Garland.

group, a sandy clay with low liquid limit and erodibility. In Duck Creek, the representative reach is located within the Ozan (Taylor Marl) Formation, near the contact of the Austin Chalk, in the Frio soil series, a very erodible silty clay with high liquid limit and plasticity index. The bottom of the reach has eroded to the underlying Austin Chalk, while the banks are still primarily Ozan. The Timber Creek reach is an alluvial channel located in the outcropping area of the Woodbine Formation, which comprises both the stream bed and banks. It is located in the highly erodible Bunyan soil, a sandy clay with

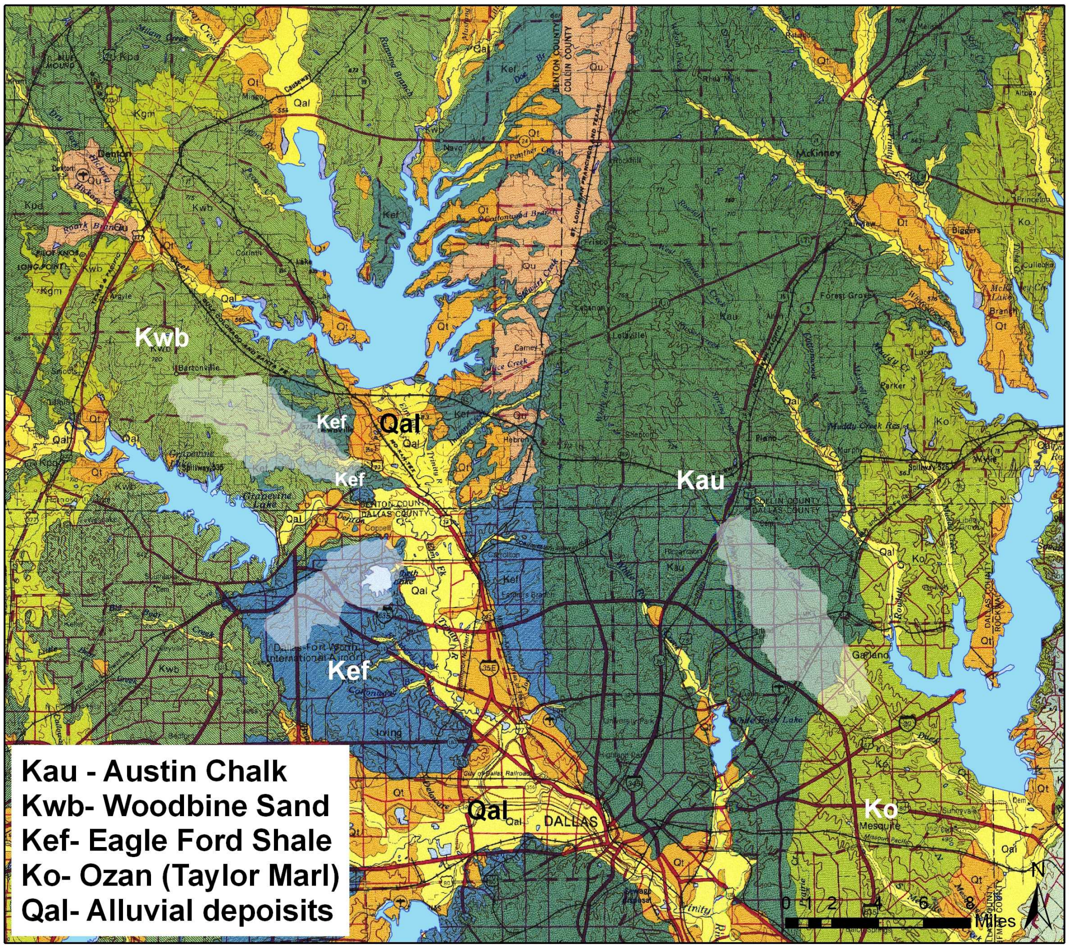

Figure 13. Geology of the Dallas area overlain with the watersheds of the three selected study areas (Geologic Atlas of Texas, 1972) All three are located, at least partially, in geologically susceptible areas. Duck Creek does overlay the Austin Chalk, but the study took place in the Ozan part of the watershed.

average liquid limit and plasticity index. Figure 14 shows the locations of these 2000 foot representative reaches within their respective watersheds, as well as the geology and soils of the reaches themselves.

The hydrologic properties of the three representative reaches include flood peaks determined by using urban flood regression equations and various channel hydrologic properties. Table 2 records the various flood discharge rates for several recurrence intervals, while table 3 provides the average annual rainfall, runoff, Manning's N

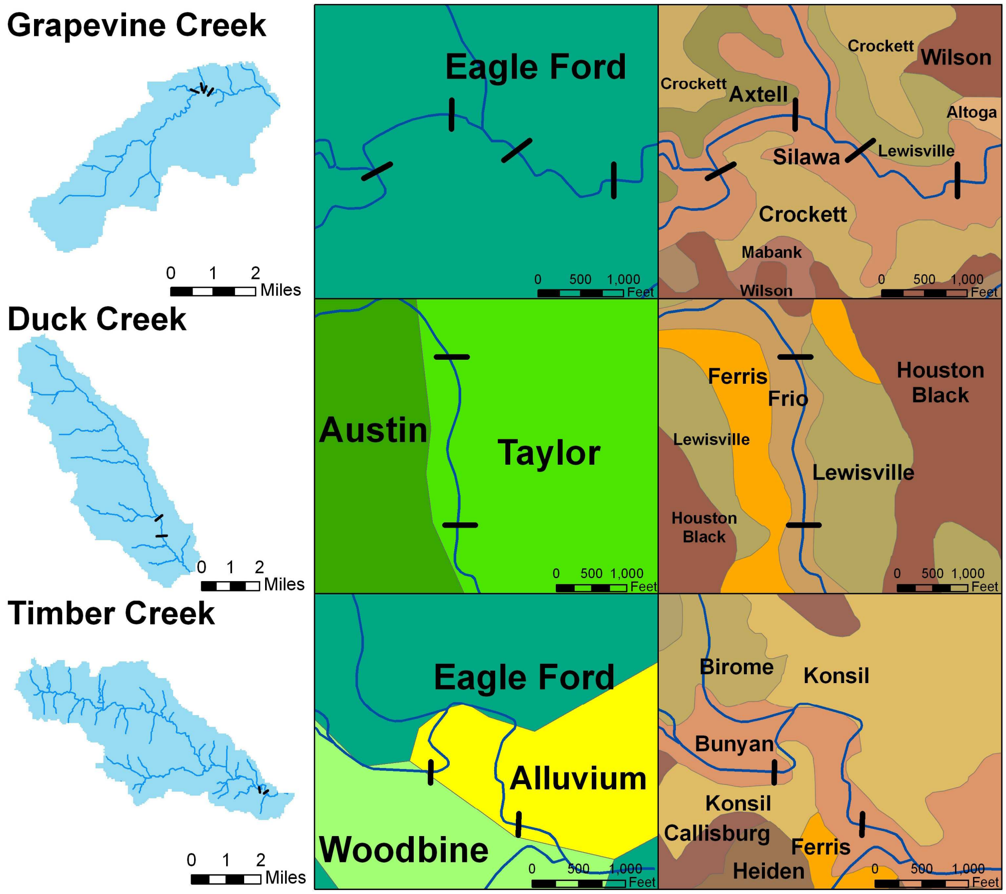

Figure 14. Overview of the geology and the soils for the 2000 foot representative reaches used in the study. Note that the Grapevine Creek study area is split into two 1000 foot segments due to the intersection of a major freeway.

Table 2. Flood recurrence intervals for the 2 to 100 year floods in the three watersheds, in cubic feet per second. (Equations from Land, 1982)

	Flood Recurrence Intervals, CFS					
Reach	2 Year	5 Year	10 Year	25 Year	50 Year	100 Year
Duck	6260	9550	11900	14900	17400	19500
Grapevine	4060	6210	7740	9760	11400	12900
Timber	5730	8710	10800	13600	15800	17700

Table 3. Basin properties for the three watersheds. Note that Duck Creek is the only watershed that is not classified as entrenched.

Reach	Basin Area (Mi^2)	Average Annual Rainfall (In)	Average Annual Runoff (In)	Manning's N	Average Entrenchment Ratio
Duck	18.7	36 - 38	7 - 8	0.035	3.31
Grapevine	11.8	34 - 36	6 - 7	0.045	2.09
Timber	16.5	35 - 36	6 - 7	0.05	2.14

(channel roughness) coefficient, and entrenchment ratio (bank width at twice the bankfull height divided by the bank width at bankfull height). Entrenchment ratios less than 1.4 are completely entrenched, from 1.4 to 2.2 are moderately entrenched, and more than 2.2 is not entrenched (Rosgen, 1994). Two of the study reaches (Grapevine and Timber) are moderately entrenched, indicating that the banks in these reaches are higher and steeper, a major consideration when calculating setback lengths.

CHAPTER TWO

Methodology

Data for the setback calculation was acquired from two sources; readily available remotely sensed elevation models and measurements obtained in the field. The data utilized include USGS 10 meter Digital Elevation Models (DEMs) and 2 foot Light Detection and Ranging (LiDAR) contour maps. DEMs were acquired from the seamless data server of the USGS and LiDAR maps were commissioned through the North Central Texas Council of Governments in February 2001 for the purpose of creating a surface profile for the entire Dallas/Forth Worth metropolitan area and the surrounding cities.

USGS DEM

USGS DEM data, as described by the USGS in their document on standards (USGS, 1997) is created on one of four levels. Level 1 DEMs are acquired from spatial auto correlation from aerial photography provided by the National High Altitude Photography Program or the National Aerial Photography Program. Level 2 DEMs utilize Digital Line Graph (DLG) contours up to 1:100,000 scale. Level 3 DEMs use DLGs that have been rectified with other data sources, such as hydrography, and Level 4 DEMs are created through electronic imaging sensor systems (i.e. RADAR). As of the publication of this report, Level 4 DEMs do not exist, but are planned for in the future, all DEMs acquired for this study were between level 1 and 3.

LiDAR

LiDAR is a new, cutting-edge technology in terms of terrain mapping (Meng, et al., 2008, *In Press*). The data are developed by the use of a laser scanner aboard an aerial platform that remotely senses the profile of the ground below at high resolution. Because of the high frequency of the laser used, data points reflected from both tree cover and the ground below can be returned. The user then has the option of using specially created interpolation algorithms to create a profile of the surface they desire, whether it be the canopy or the ground surface (Bater and Coops, 2008; Charlton, et al., 2002). Following post processing, accuracy of such LiDAR platforms can average to .274 meters (.90 feet) vertically (Vaze and Teng, 2007).

Field

The field testing measured similar parameters; bank width and side slope, at an interval of approximately 50 feet along the study reach. Bank angles and widths were taken with a bank inclinometer and a laser range finder at each cross section. Differentially corrected handheld GPS was also used to mark the exact location for each measured cross section to coordinate the field cross section intervals with the DEM and LiDAR created cross-sections.

Aerial photography from the National Agriculture Imagery Program (NAIP, 2005) provided a visual background for the setbacks. The false infrared imagery allowed for easy detection of structure location on the study sites. By rendering the images with the stream centerlines, the extents of the setback buffers were assessed.

Data Processing

The DEM and LiDAR data was extracted using the HEC-GeoRAS application from the US Army Corps of Engineers (Cameron and Ackerman, 2005). The HEC-GeoRAS application extracts stream cross sections at user-defined intervals by analyzing an input elevation raster. The stream centerline and bank lines are also calculated within the program. The program accepts both grid formats and triangular irregular network (TIN) files. TINs, which characterize surfaces through source point interpolation (Lo and Yeung, 2007), are easily created from raw LiDAR data; however, since the readily available LiDAR data was provided as contour lines, a grid surface with a cell size of 5 feet was created for the analysis. The DEM data was provided as a grid, and required no conversion.

The cross section interval must be determined in HEC-GeoRAS before the analysis, as it can be adjusted to coincide with the user's desired resolution and method for drawing setbacks. Users can draw setbacks either by connecting the points representing the perpendicular setback distance from the stream centerline or by using a tool to draw a semi-circle with a radius equal to the setback distance and center at the stream centerline. For this analysis, circular buffers were chosen as the method of drawing the setbacks. By using spacing equal to one quarter of the diameter of the eventual setbacks, the overall difference between chords and arcs in the circular buffers is 0.2%. Because the streams surveyed in this study average 100 feet in width, and we can expect these streams to enlarge 2 to 3 times (Chin, 2006), the minimum interval should be every 50 feet (one quarter of 200 feet). With this interval, and representative reaches of 2000 feet, approximately 40 cross sections were created for each watershed for each method.

Setback Calculation

The "setback zone" describes the area of the stream corridor that is susceptible to erosion and stability problems. This is based on the research by Schumm (1999) and

Simon and Hupp (1986) into bank erosion processes. Previous research on calculating setbacks is provided by the City of Dallas ordinance 51A-5.106, the engineering firm Ayres and Associates (2004) and Cruden (1989), whose methods are shown (Fig. 15). The Dallas ordinance specifies a setback as the lateral distance defined by the intersection of a line extended from the toe of the bank to the top of the bank or floodplain at 4 horizontal to 1 vertical in shale or clay and in limestone, the setback is calculated as a line projected from the toe of the bank at 3 horizontal to 1 vertical. The Cruden setback calculates the setback from the toe of the bank, adjusted for lateral erosion distance. A line is then projected from the toe at the angle of ultimate stability, the angle at which the bank material is assumed stable from slope failures. The setback defined by Ayres and Associates calculates the setback as the angle stretching from an elevation from the toe of the bank, adjusted for downcutting (three times the bankfull height), at an angle of 6 horizontally to 1 vertically in alluvium, 4.5 horizontally to 1 vertically in bedrock, and a combination of the two if there is alluvium above bedrock.

Because this research focuses on urbanizing watersheds that typically degrade and widen, the setback algorithm by Ayres and Associates (2004) for the City of Austin is used. Additionally, in this research, the algorithm will be constructed with the user option of changing the setback angle based on local knowledge of bank stability.
The downcutting depth is defined in the setback as three times the bankfull height (Ayers and Associates, 2004) and is utilized here. The average bankfull height in streams is defined by Dunne and Leopold (1978) as the depth of the 1.5 year flood recurrence interval. A conservative approach for this region used the 2 year flood as defined by Land's (1982) regression equation specifically created for urbanized Dallas/Fort

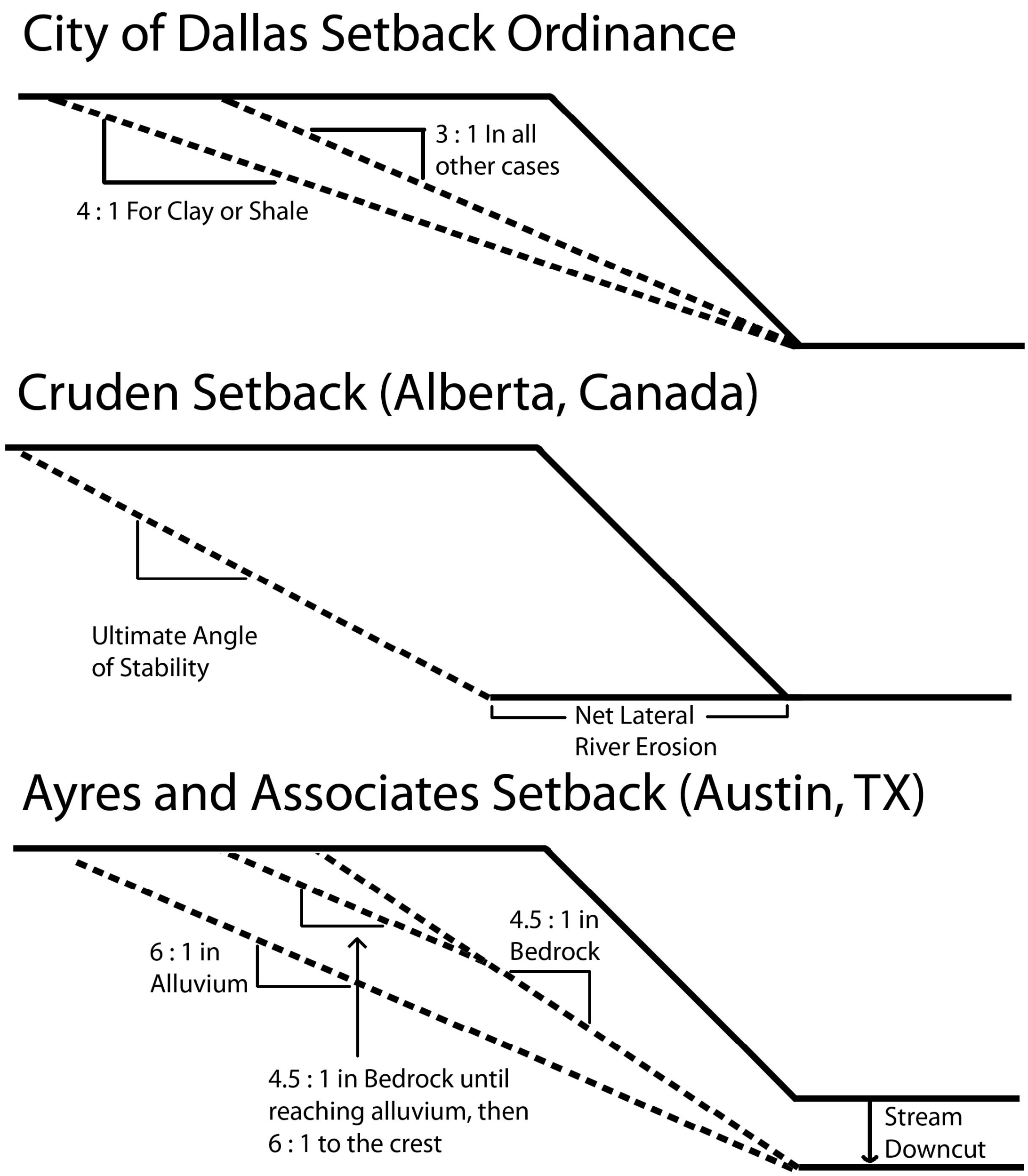

Figure 15. Comparison of three different methodologies for calculating setbacks. The Dallas and Austin setbacks utilize a fixed angle for the setback, while the Alberta setback requires a stability angle calculated by bank material and other parameters. The Austin setback also incorporates a downcutting component, making it ideal for stage II and III CEM analysis.

Worth streams:

$$Q_2 = 42.83\ (A)^{.704} * (UI) * .836 \qquad (1)$$

Where Q_2 is the two year peak discharge, A is the basin area in square miles and UI is the urbanization index (Land et al., 1982). Land's urbanization index is calculated by determining the overall prevalence of storm sewers, channel rectifications and curbs/gutters within the watershed (Table 4). By assigning a score for each category based on the percentage of the subbasin affected, and repeating the process for the lower, middle and upper regions of the watershed, a value between 9 and 33 is produced for the calculation.

Table 4. Land's (1982) urbanization index is based on how much of the subbasin is affected by the urbanization factors. This process is repeated three times, on the upper, middle, and lower portion of the watershed, so values for UI can range from 9 to 36.

	Percent Covered			
Urbanization Factor	0% - 24%	25% - 49%	50% - 74%	75% - 100%
Storm Sewers	1	2	3	4
Curbs and Gutters	1	2	3	4
Channel Rectifications	1	2	3	4

The peak discharge acquired from the regression equation is then used in Manning's (1851) Equation:

$$Q = VA \qquad (2)$$

$$V = (K/N) * (A/P)^{2/3} * S^{1/2} \qquad (3)$$

Where Q is the peak discharge, V is velocity, A is cross sectional area, P is the wetted perimeter, S is channel slope, N is Manning's N coefficient and K is a metric to English unit conversion factor. By backsolving this equation for wetted perimeter (P)

(Daugherty, et al. 1985), a bankfull height can be calculated. This volume is subsequently multiplied by three to get the downcutting depth for the setback. The angle used for the analysis differs based on bank composition, usually set at 4.5:1 for bedrock channels, 6:1 for alluvial channels, and a combination of the two angles for composite channels. (Aryes and Associates, 2004).

The actual horizontal distance of the setback zone is then calculated individually for both right and left sides by:

$$((H_b + H_d) / \tan\theta_s) + ½ * W_b \quad (4)$$

Where H_b is the bank height, H_d is the downcut height, θ_s is the setback angle, and W_b is the channel bottom width. The formula assumes that the user is measuring setback distance from the center of the stream. If the user wishes to draw the setback from the toe of the bank, W_b can be removed.

In equation (4), it is assumed that the bank angle is steeper than the setback angle. This implies that the setback will extend further than the top of the bank (Fig. 16). If this is not the case, the setback angle will intersect with the bank before reaching the floodplain (Fig. 17) and a different equation must be used. This setback is defined by an alternate equation:

$$(H_d / (\tan\theta_s - \tan\theta_b)) + ½ * W_b \quad (5)$$

Where H_d is the downcut height, θ_s is the setback angle, θ_b is the bank angle and W_h is the bank width.

The process of calculating these setbacks was automated using Microsoft Excel. This allows the user to perform multiple setback calculations in a short amount of time. The formula setup of this spreadsheet is given in the appendix.

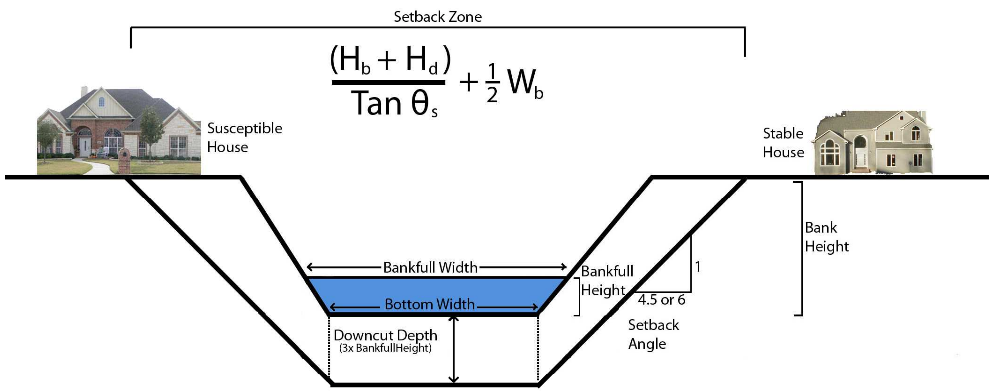

Figure 16. Setback calculation for when the setback angle intersects with the ground after the crest of the bank.

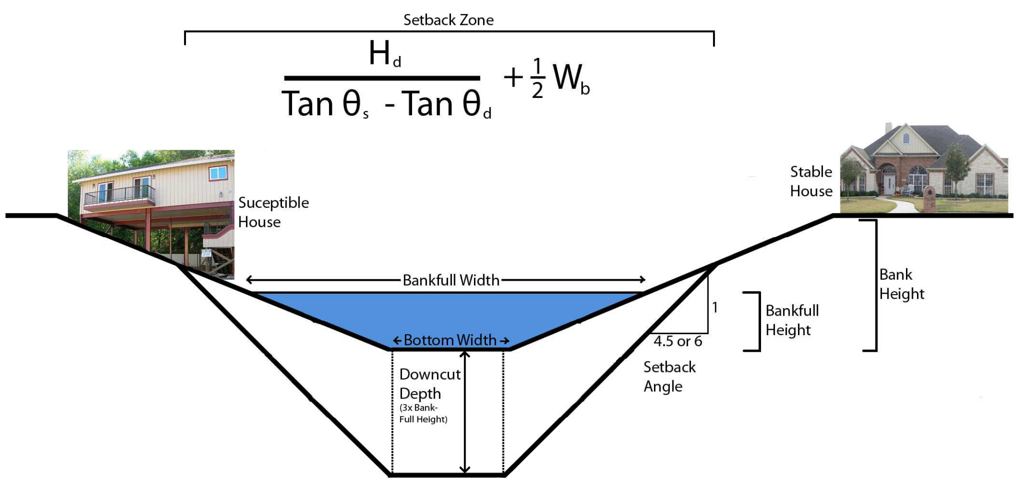

Figure 17. Setback calculation for when the setback angle intersects with the ground before the crest of the bank.

The setback corridor along a stream is then calculated by stringing multiple setbacks together. The data acquired from the cross sections is loaded into the setback calculations. The setbacks are then be drawn perpendicular to the stream and connected with the neighboring cross sections' setback to create a setback corridor. These corridors can be drawn on top of aerial images to calculate how many structures fall into each corridor. The corridors created by different methods are also compared to each other.

Channel slope and basin drainage area were calculated for each individual study reach using USGS topography maps. These parameters remained unchanged for each study reach throughout all 3 methods. The HEC-GeoRAS program extracted cross sections from each reach using both DEM and LiDAR data. This data was used to calculate the values to input to the setback algorithm; bank width, side slope angles and side slope elevation changes. Similarly, field data was compiled at each cross section and the same parameters extracted for use in the setback algorithm for comparison to the remote methods.

The setback algorithm was developed through the use of a Microsoft Excel spreadsheet. By utilizing the previously stated equations, the program is capable of determining the setback distance, in feet, for each cross section. The required inputs are channel slope, bottom width, right and left elevation change and length, 2 year flood velocity (as defined by Land's (1982) regression equation) and Manning's N. The user must also define which setback angle they wish to use; in this case, 6:1 was used as channels were mostly alluvial. The algorithm then calculates all remaining variables, including both setback equations before automatically determining which setback scenario is appropriate for the result. These setback values used to construct the setback buffer zones.

CHAPTER THREE

Results

Because the field data represents the most accurate input parameters to the setback algorithm, the setbacks defined by this dataset will be used to compare the accuracy of the results acquired from the computed DEM and LiDAR setbacks. Setbacks and inputs to the setback algorithms were compared in several ways; (1) several of the acquired parameters to the setback algorithm were compared for their relative accuracy (Fig. 18, tables 5 - 7), and (2) cross sections of the resulting setback zones were measured and compared (Fig. 19, tables 8, 9).

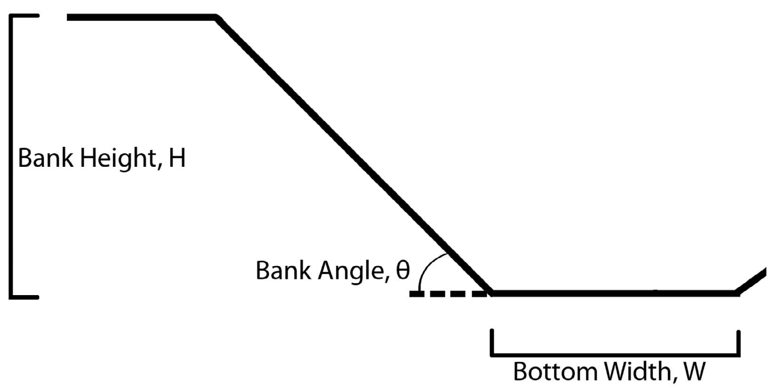

Figure 18. For each method, the extracted bank width, bank angle and bank height were compared to each other for accuracy. The values are reported in table 8, while the comparison of the field values to the DEM and LiDAR values are reported in tables 9 and 10, respectively.

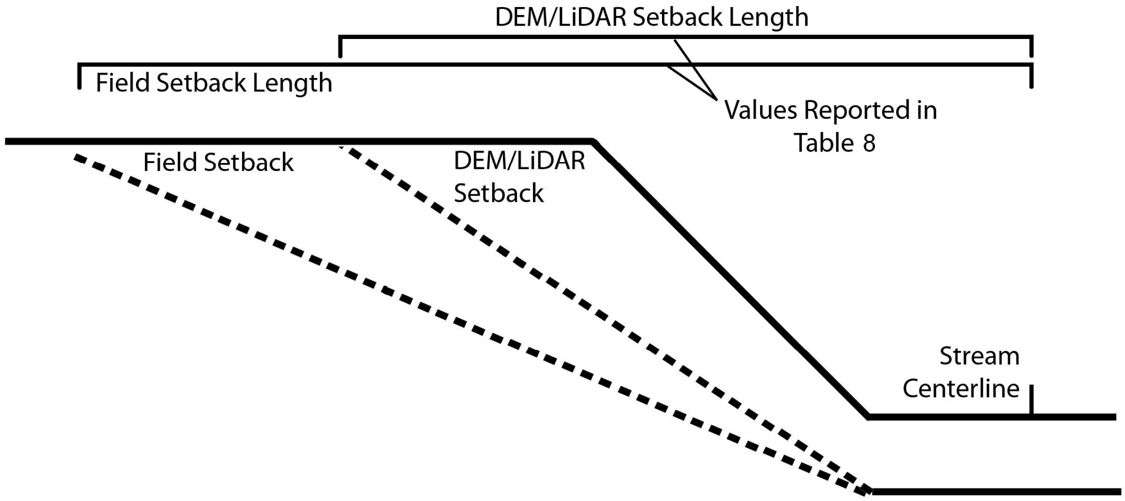

Figure 19. For each method, cross sections were taken of the setback buffers, measured as the distance from the stream centerline to the buffer's edge. The differences in length for each method are reported in table 8.

Table 5. Averages of the major input parameters to the setback algorithm for each method.

	Field Measurements			DEM Measurements			LiDAR Measurements		
Reach	Bottom Width, Feet	Average Elevation Change, Feet	Average Bank Slope, Degrees	Bottom Width, Feet	Average Elevation Change, Feet	Average Bank Slope, Degrees	Bottom Width, Feet	Average Elevation Change, Feet	Average Bank Slope, Degrees
Grapevine Creek	18.28	17.07	34.79	91.30	17.94	5.04	34.80	16.71	11.41
Timber Creek	19.33	16.02	37.89	65.90	6.86	3.43	26.90	16.78	10.95
Duck Creek	13.74	15.25	17.50	48.70	18.00	13.49	48.70	11.60	13.49
Averages	17.12	16.11	30.06	68.63	14.27	7.32	36.80	15.03	11.95

Table 6. Comparison of the major input parameters acquired in the field to the ones derived from DEM cross-sections.

Reach	DEM versus Field					
	Bottom Width Difference		Average Elevation Difference		Average Bank Slope Difference	
	Feet	Percent	Feet	Percent	Degrees	Percent
Grapevine Creek	63.66	399%	0.86	5%	-29.75	86%
Timber Creek	41.04	241%	-9.16	57%	-34.46	91%
Duck Creek	82.05	254%	-3.66	18%	-13.68	23%
Averages	62.25	298%	-3.98	27%	-25.96	66%

Table 5 provides the average bottom width, bank height and bank angle input into the setback algorithm. For example, the field derived bank width average for Grapevine Creek is 18.28 feet, the average elevation change from the bank to the stream bottom is 17.07 feet, and the average bank angle was 34.79°. The same measurements are repeated for DEM and LiDAR. The overall differences in these variables are compared in

Table 7. Comparison of the major input parameters acquired in the field to the ones derived from LiDAR cross-sections.

Reach	LiDAR versus Field					
	Bottom Width Difference		Average Elevation Difference		Average Bank Slope Difference	
	Feet	Percent	Feet	Percent	Degrees	Percent
Grapevine Creek	7.16	90%	-0.37	2%	-23.38	67%
Timber Creek	2.03	39%	0.76	5%	-26.94	71%
Duck Creek	-22.86	254%	2.75	24%	-4.01	23%
Averages	-4.56	128%	1.05	10%	-18.11	54%

Table 8. Comparison of the average cross-sectional setback length for each watershed for each method.

Reach	Average Setback Length				
	Field	DEM		LiDAR	
	Length, Feet	Length, Feet	% Difference from Field	Length, Feet	% Difference from Field
Grapevine	320.2	199.3	38%	246.4	23%
Timber	334.2	171.6	49%	249.4	25%
Duck	240.7	170.0	29%	311.2	29%
Average	298.4	180.3	39%	269	26%

Table 9. Comparison of the total area of the setback zone, in acres, per creek per method.

Reach	Overall Setback Size				
	Field	DEM		LiDAR	
	Size, Acres	Size, Acres	% Difference from Field	Size, Acres	% Difference from Field
Grapevine	30.40	18.48	39%	23.67	22%
Timber	39.32	18.89	52%	30.33	23%
Duck	26.21	18.04	31%	33.38	27%
Average	31.98	18.47	41%	29.13	24%

table 6 (DEM versus field data) and table 7 (LiDAR versus field data). For example, in Grapevine Creek, the DEM measured bottom with is 63.66 feet greater than the field data, or 399% different. The DEM data overestimated the elevation change by .86 feet, or 5%, and the bank slopes were 29.75° less, or 86% off. Table 8 compares the average length of the setbacks for each method, with a percent difference to the field data for the DEM and LiDAR derived lengths. For example, the field data in Grapevine Creek provided an average setback length of 320.2 feet. The DEM derived setback corridor in that reach was, on average, 199.3 feet wide, or 38% off. The LiDAR corridor was 246.4 feet wide, only 23% off. Finally, in table 9, the overall areas of the setback buffer zones,

in acres, are recorded for each method, with a percent difference from field for the DEM and LiDAR derived buffers. For example, in Grapevine Creek, the setback corridor provided by the field data was 30.40 acres in size, whereas the DEM corridor was 18.48 acres, a 31% difference, and the LiDAR was 23.67, a 22% difference.

The DEM derived setback corridors greatly underestimated the field data in all three watersheds, primarily due to the differences in bank parameters acquired from the DEMs. Because of the overestimated bank widths and the underestimated bank slopes in all three cases, the setback corridors averaged much smaller, 180.3 feet across, on average, as opposed to the field average cross section length, at 298.4 feet. The maps comparing the overall size of the three DEM corridors to the field data are shown in figures 20 - 22.

The LiDAR derived setback corridors were much closer to the field derived setbacks. The input parameters to the setback algorithm were much closer to their respective field values. While bank slope was still greatly underestimated, the values were actually closer than the DEM derived counterparts. Average cross sections of the setbacks were 269.0 feet, much closer to the field value than the DEM corridor. The maps comparing the LiDAR corridors to the field data are shown in figures 23 - 25.

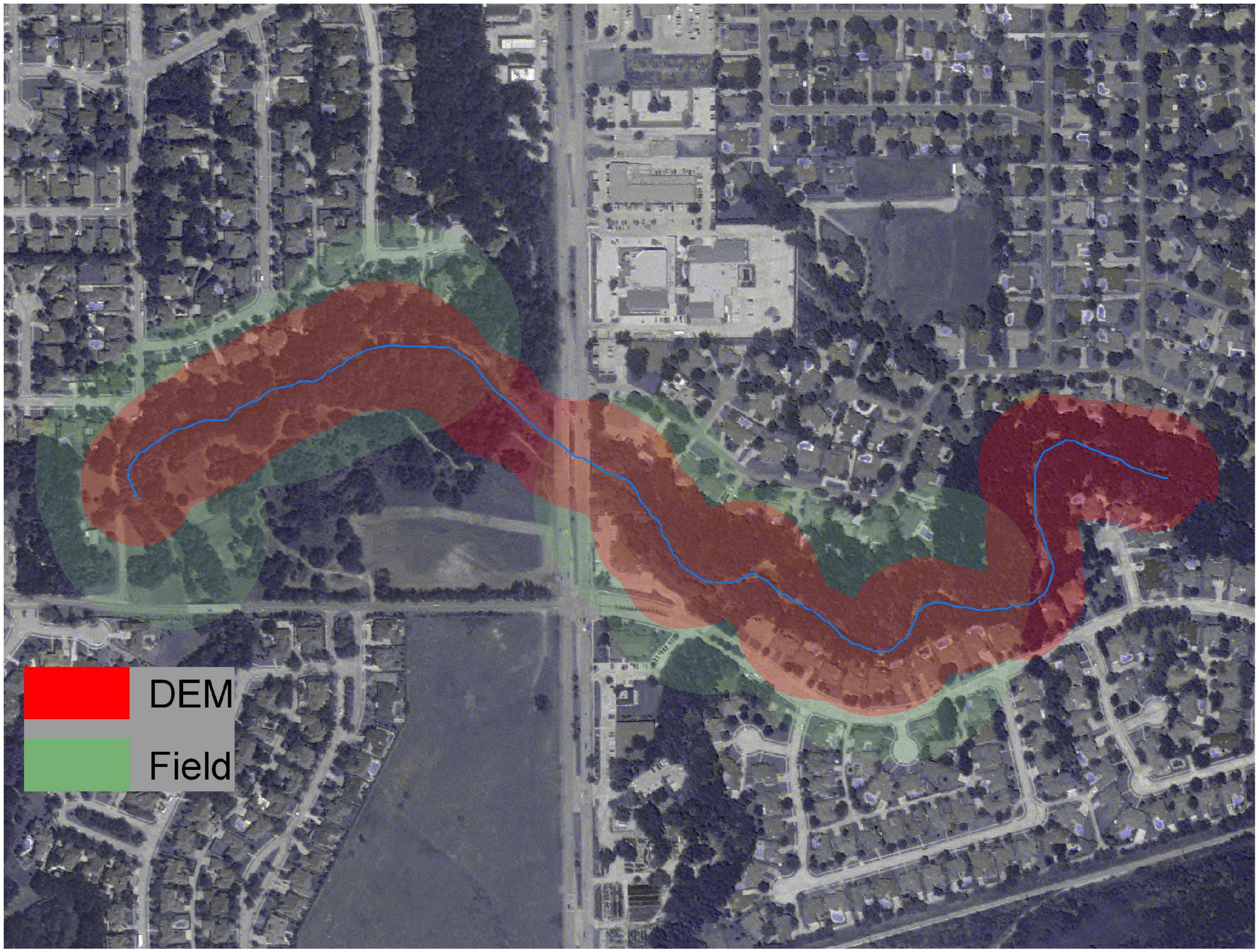

Figure 20. The DEM derived setback corridor compared with the in-situ generated setback corridor for Grapevine Creek in Coppell, Texas.

Figure 21. The DEM derived setback corridor compared with the in-situ generated setback corridor for the Timber Creek study area in Lewisville, Texas

Figure 22. The DEM derived setback corridor compared with the in-situ generated setback corridor for Duck Creek in Garland, Texas.

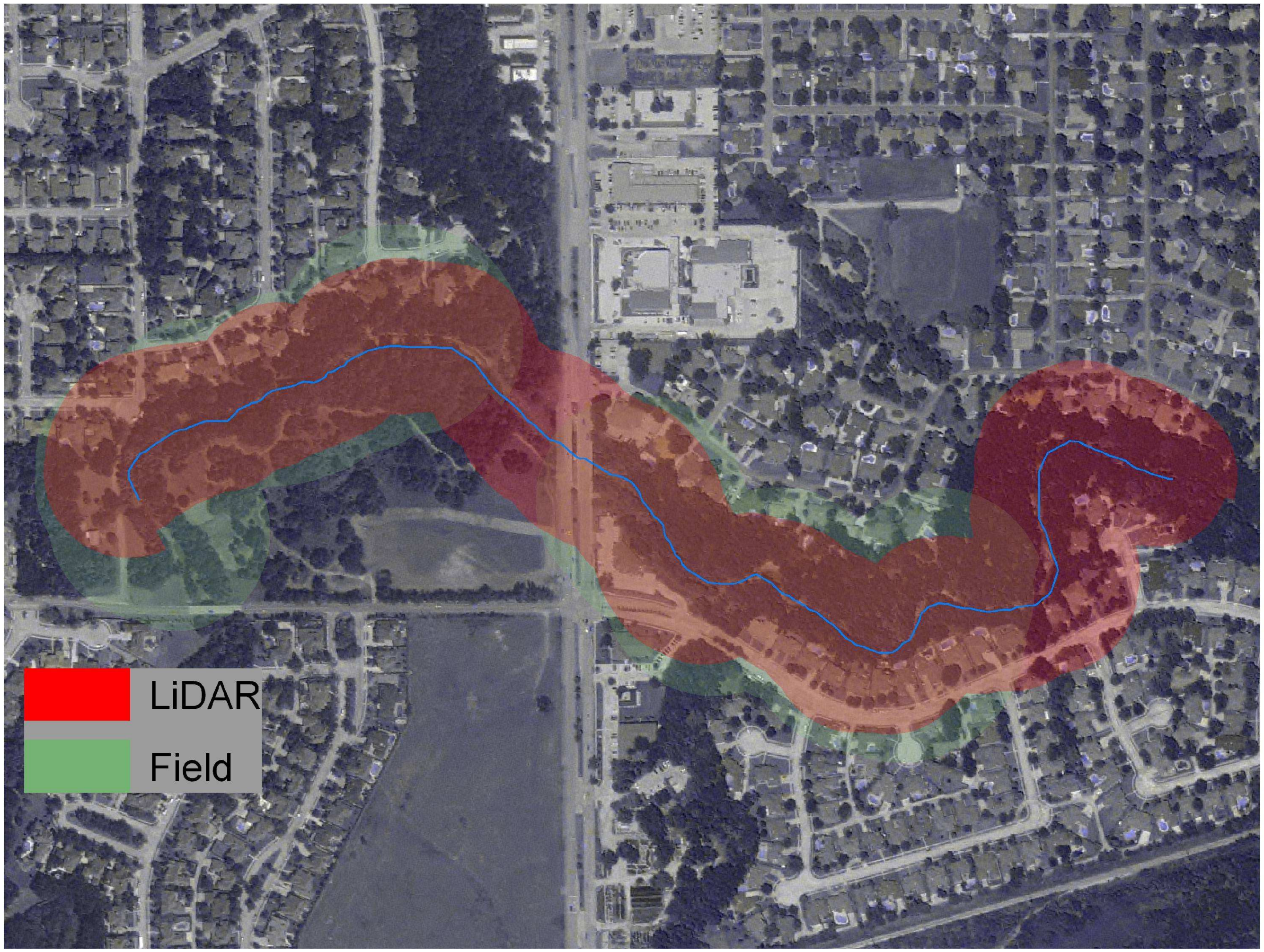

Figure 23. The LiDAR derived setback corridor compared with the in-situ generated setback corridor for Grapevine Creek in Coppell, Texas.

Figure 24. The LiDAR derived setback corridor compared with the in-situ generated setback corridor for the Timber Creek study area in Lewisville, Texas.

Figure 25. The DEM derived setback corridor compared with the in-situ generated setback corridor for Duck Creek in Garland, Texas. Note that this is the only instance where the LiDAR setback is larger than the field calculated setback.

CHAPTER FOUR

Discussion

The two main goals in this study were to first develop a method of extracting cross sectional data and secondly, developing a simple, user friendly algorithm into which the acquired data can be entered. Both goals were adequately met in the course of this research; however, each method (DEM, LiDAR and in-situ) provided a slightly different setback. The following discussion assesses reasons why the differences occurred and recommend which methods should be used when this algorithm is utilized for planning purposes.

The Setback Algorithm

Utilizing the equations in the algorithm, a Microsoft Excel worksheet has been created that clearly labels the required inputs and solves for the setback lengths. It is unlikely that any variation between the three methods of data acquisition is the result of the algorithm itself, as any mistake in the writing of the formulas would affect all three results relatively equally. Therefore, the variation of the three methods is thought to be attributable to the data.

USGS DEM

Because of the nature of aerial photo and/or topographic map derived level 1, 2 or 3 DEMs, overall accuracy of the DEMs used in this study are questionable. All three levels of DEM rely on autocorrelation, or the assumption that the elevation data will not make sudden changes (USGS, 1997). This can lead to underestimated channel depths, leading to side slope calculations that are not as steep as they are supposed to be, as well as cliff sides that are completely smoothed over by autocorrelation. Also, DEMs acquired in this fashion are generally incapable of capturing geomorphologic features with any kind of accuracy (Rayburg, et al., 2008, *In Press*). Additionally, when aerial photography platforms are used, most creeks and streams will have a riparian buffer zone consisting of large trees that can obstruct the bank edges from view, which is another potential source of error. The overall vertical accuracy of DEM data is another potential source of error; a comparison of 13,305 geodetic control points to DEM data showed that DEM data had an average vertical difference of 1.64 meters (5.39 feet) (Gesch, 2007). Vertical disparity of this magnitude is capable of shifting setback calculations 15 to 25 feet.

Overall confidence in the accuracy of DEM-derived setbacks buffers is questionable. Methods of DEM creation were designed to work on large watershed scale projects and not small urban streams. The resolution of the available source DEMs contributing to cross-section data with HEC-GeoRAS is marginal. The HEC-GeoRAS program extracts cross sections by plotting cross section points graphically as the cross section 'cutline' crosses a DEM grid cell. Because of the 10 meter resolution, in some cases, as few as 12 points were used to represent a single cross section, or only 6 points were used to calculate bank side slope for either side. Figure 26 shows an example cross section extracted from a DEM surface and the resulting cross section profile used in the HEC-GeoRAS program. With such a small amount of sample points available, the data is susceptible to error simply due to poorly defined side slopes within the HEC-GeoRAS program. Therefore, because of the potential for errors associated with using this kind of data, it is not recommendable to use 10 meter DEM data for this purpose.

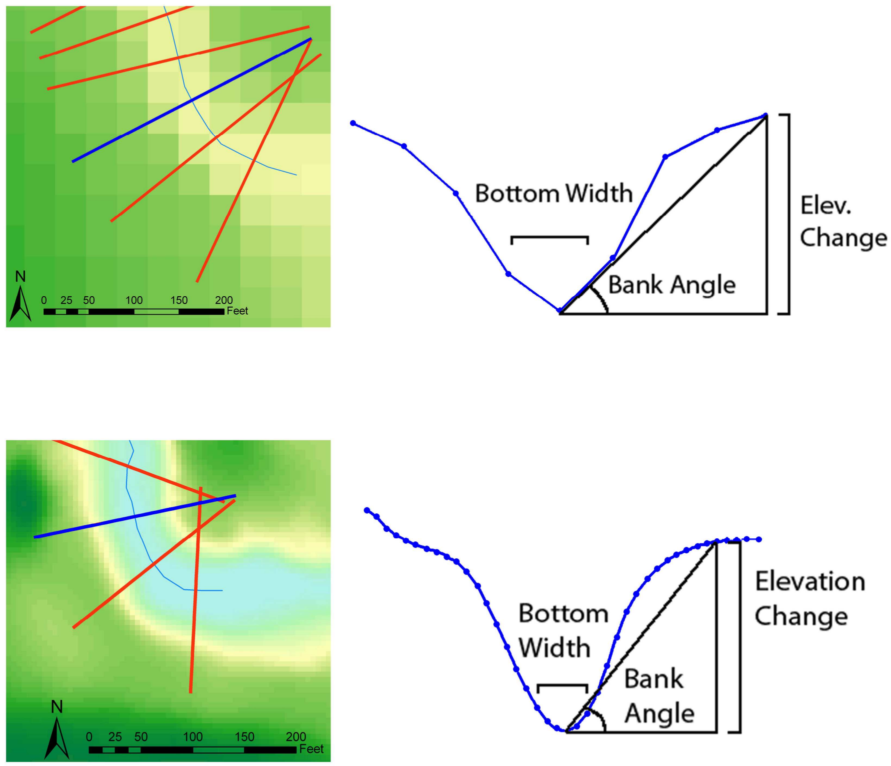

Figure 26. Comparison of the cross-sections HEC-GeoRAS derived from the two surfaces. DEMs (above) are more pixilated at this zoom level, and therefore do not lend many points to the cross section interpretation. LiDAR-derived surfaces (below) are more precise, allowing for a better cross section. The cross sections seen here are taken from approximately the same location on Timber Creek.

LiDAR

The available LiDAR data is technically superior to the 10 meter DEM. The resolution of the LiDAR generated grid is 5 feet (1.52 meters), or six times more detailed than the 10 meter DEM. This allows the HEC-GeoRAS program to extract much more detailed cross sections or up to 40 points per cross section (fig 26). Additionally, smoothing algorithms can be used in LiDAR to reduce error from riparian cover (Bater and Coops, 2008). However, these algorithms assume that abrupt changes in terrain elevation are the result of internal error or interference and smooth them (Meng, et al. 2008). This can be detrimental to the setback algorithm used in this research. In some instances, near vertical slopes are completely disregarded by the LiDAR data (Fig. 27). Here, a near vertical slope measured in the field is calculated to be 24° according to the LiDAR contour lines. This LiDAR smoothing function can lead to setback results that are on average 80 feet shorter than the ones calculated in the field.

Therefore, despite it being a far superior product than the USGS 10 meter DEM data, LiDAR data may not be an acceptable alternative to field data. If LiDAR data is used for this purpose, access to raw data may allow the user to find and correct areas where smoothing algorithms have distorted the true surfaces. Otherwise, in-situ field testing will be needed, especially in areas of dense vegetation and steep slopes.

Field Data

The field data was collected using several basic surveying tools; a digital range finder, accurate to within one meter, was used to calculate stream bottom widths and bank heights, while an inclinometer was used to calculate the bank angle. In Grapevine and Timber Creeks, the foliage was sparse enough to accurately estimate the bank heights with the range finder, however, in Duck Creek, more dense vegetation made it difficult to estimate bank angles and bank heights in small sections of the reach, which may have skewed the data slightly. However, since there were no major outliers in the resulting setback corridors, the estimations in these areas are assumed to be within tolerance. Despite the technical difficulty surrounding Duck Creek, the field data represents the most accurate estimates of the setback calculations, at the expense of being the most

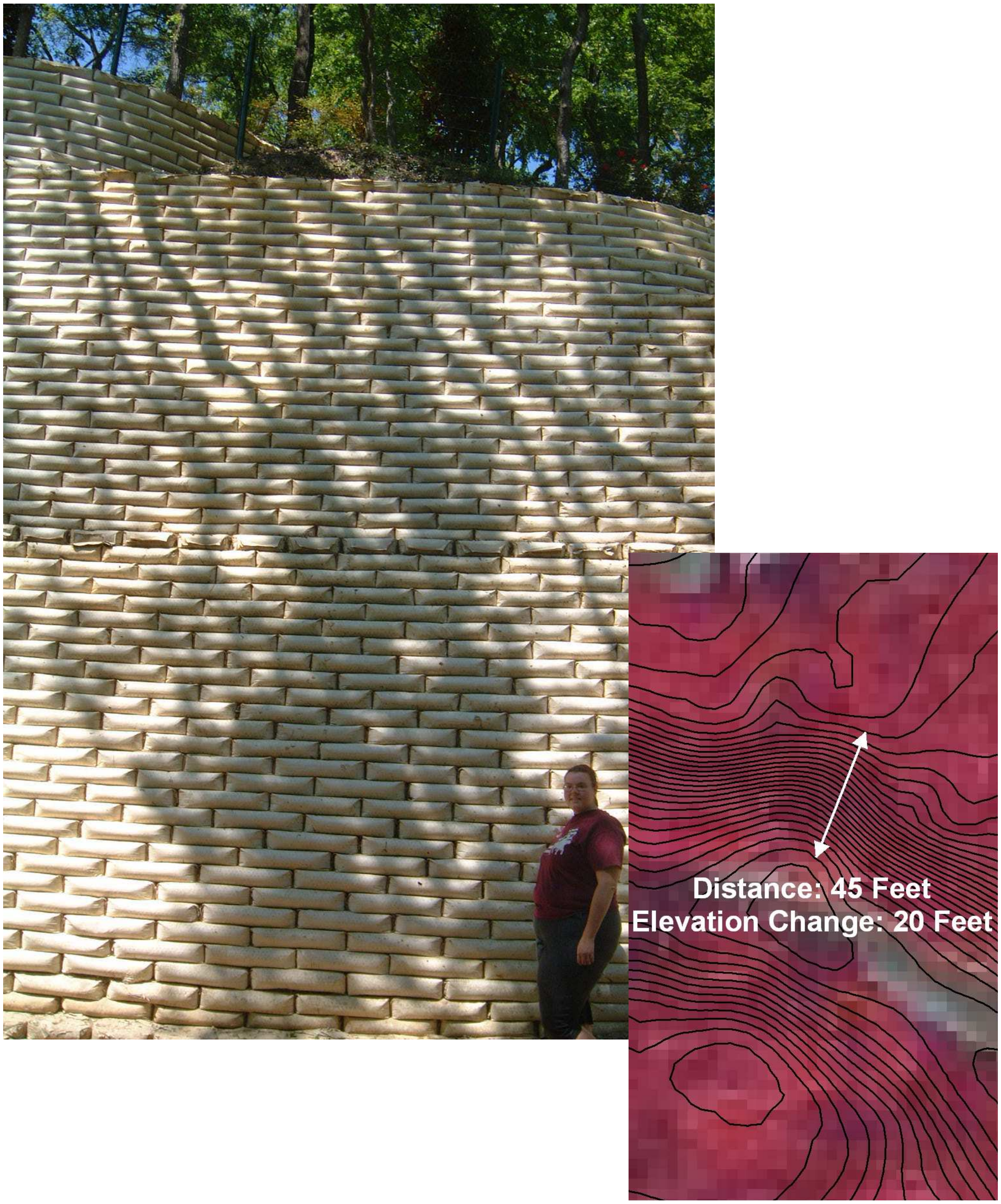

Figure 27. In the image, the wall is approximately 30 feet tall at an angle of 82.5°. The same geographic location, according to the LiDAR data, is 24°.

tedious method of data collection, up to 2 hours per 2000 foot reach with a two man crew. The ultimate objective is to create a methodology that will minimize field checking in the future. However, that may not be possible unless a reliable way of removing error associated with smoothing algorithms is developed. Until then, field checking of areas with known dense vegetation or areas with steep slopes should be checked as a supplement to automated setbacks.

Potential Impact

In all three watersheds, a significant number of structures were located within the setback zone acquired from the field data. Almost every house along the bank was within the setback zone, and, in some cases, the setback zone stretched across neighborhood streets. In total, 161 structures fell into the setback zones of the study reaches, with the potential for more, as a small section of Grapevine creek is currently undergoing construction for residential housing.

Table 10 records the precise number of houses for each study reach that are within the setback zone, the amount that are in need of stabilization and the number of houses that have already attempted to stabilize the bank with gabions or gunite coatings. Each category was divided by the total length of the banks to determine houses per bank foot. For example, in Timber Creek, 64 houses are in the setback zones, or .016 per bank foot. 4 houses need stabilization (.001 per bank foot) and no houses are stabilized. In Table 11, the values for the three reaches are averaged, and by using the houses per bank foot parameter, it is shown that along any given mile of stream bank, 71 houses will be in the setback zone, or one house per 74.5 feet. Table 12 provides an estimate for the cost of a typical repair, depending on the length of the property and the height of the bank at the property line. The cost for a single lot ranges from $25,000 to $75,000 to repair, meaning that for a single mile of unstable stream bank, homeowners could collectively pay between $275,000 and $825,000, or about $156 per foot of river.

Table 10. Report on how many structures from each watershed fall into the setback zone, how many are in immediate need of stabilization, and how many have already been stabilized through methods such as gabions.

	Timber Creek		Duck Creek		Grapevine Creek	
Situation	Number of Houses	Houses per Bank Foot	Number of Houses	Houses per Bank Foot	Number of Houses	Houses per Bank Foot
In Setback Zone	64	0.016	57	0.01425	40	0.01
Need Stabilization	4	0.001	11	0.00275	10	0.0025
Stabilized	0	0	5	0.00125	9	0.00225

Table 11. Report on the average number of houses in each situation per bank foot and per bank mile, as well as how many feet per house.

Average Houses…	Number	Houses Per Bank Foot	Houses Per Bank Mile	Feet Per House
In Setback Zone	54	0.0134	71	74.5
Need Stabilization	8	0.0021	11	480.0
Stabilized	5	0.0012	6	857.1

Table 12. A look at how much stabilization of degrading bank property can be.

Hypothetical Parameters				
Length of Property at the Bank	100 Feet	100 Feet	150 Feet	150 Feet
Height of the Bank Behind the Property	5 Feet	10 Feet	5 Feet	10 Feet
Cost of Repair Per Square Foot (Allen, 2009)	$ 50	$ 50	$ 50	$ 50
Total Cost for Repair	$ 25,000	$ 50,000	$ 37,500	$ 75,000
Cost Per Mile -	$ 275,000	$ 550,000	$ 412,500	$ 825,000

CHAPTER FIVE

Conclusion

USGS 10 meter DEM data should definitely not be used for any analysis of setbacks. All setback calculations made with the DEM data yielded significantly smaller setback zones than both LiDAR and field data. Additionally, two-tailed t-testing of the mean setbacks revealed that they are significantly different from the field data at α =.05.

LiDAR estimates are within 26% of the total setback zone area, based on the field setback area for all three watersheds. The fact that the setback zones are 26% or 29.4 feet off from the field data is not ideal; in fact, t-testing still ranked it as significantly different at α =.05., but it could be close enough to allow users to utilize LiDAR data as a first order approximation for their setback zones. After using the setback algorithm in conjunction with LiDAR data, the user could then decide either to expand the setback zone equally in all directions by 26% to create a relatively conservative corridor, or send a small team into the field to check for potential sources of error (i.e., smoothed cliff sides) in the data. Future research in this field should probably look for methods of rectifying smoothing error made by LiDAR data and quantifying the error with topography.

Regardless of the source of the input data, a setback algorithm has been produced from this research, and it is capable of rapidly creating setback corridors from the input data. This tool will most certainly assist engineers and planners in the future as they attempt to create setback corridors on their own watersheds using their own parameters.

Finally, failure to approve setbacks will cause a significant financial burden, as homeowners with slope stability problems in their back yard may choose to simply relocate instead of dealing with costly restoration measures, causing cities to lose its tax base. Setbacks will prevent this situation, keeping both homeowners and local governments from having to deal with incising channels.

APPENDIX

Formulas in the Setback Algorithm

Table A. 1. The setback algorithm as it appears in Microsoft Excel™. The columns are broken into several segments, A – J and K – N below, M – T and U – X on the following page and Y – AB on the following page.

A	B	C	D	E	F	G	H	I	J
Basin Parameters		Basin Area (Square Miles)	10		2 Year Flood (Cubic Feet/Sec)	4000			
		Slope (ft/ft)	0.00243309						
		Slope (ft/mi)	1.411765						
	Input	Input	Input	Input	Input	Input	Input	Solved	Input
Cross Section #	Bottom Width (Feet)	Setback Angle	Left Elevation Change (Bank to Thalweg)	Left Elevation Length	Right Elevation Change (Bank to Thalweg)	Right Elevation Length	Manning's "N"	Bankfull Water Height	Velocity (CFS)
1	128.45	12.52	21.71574148	186.95	12.7675003	184.6	0.045	5.206784085	4000
1	128.45	12.52	21.71574148	186.95	12.7675003	184.6	0.045	5.206784085	G3

K	L	M	N
Solve For			
Use the Excel Solver to solve this for the number in Cell J by Changing Cell I	CS Area (Square Feet)	Velocity (Ft/Sec)	Hydraulic Radius
4000	981.499	4.075	3.94
(1.49/H)*((B+(P*I))*I)*(((((B+(P*I))*I))/(B+(2*(SQRT((P^2)+1)*I))))^(2/3))*(D4^0.5)	(B+P*I)*I	J/L	(((M/((1.49/H)*(D4^0.5)))^1.5))

O	P	Q	R	S	T
Wetted Perimeter (Feet)	Average Side Slope	Bankfull Width (Feet)	Downcutting (Feet)	Left Bank Angle	Right Bank Angle
249.0	11.53	120.443	15.620	6.63	3.96
L/N	(AVERAGE((E/D),(G/F)))	O-(B+((I)/(90-SIN((S)*PI()/180)))+((I)/(90-SIN((T)*PI()/180))))	I*3	90-(ATAN((E/D))*180/PI())	90-(ATAN((G/F))*180/PI())

U	V	W	X
All Setback Calculations in Feet			
Left Setback 1	Left Setback 2	Right Setback 1	Right Setback 2
232.3594692	211.7219336	192.0631332	166.3870097
((D+R)/(TAN(((C)*PI()/180))))+(0.5*B)	((R)/((TAN(((C)*PI()/180)))-((TAN(((S)*PI()/180))))))+(0.5*B)	((F+R)/(TAN((C*PI()/180))))+(0.5*B)	((R)/((TAN((C*PI()/180)))-((TAN((T*PI()/180))))))+(0.5*B)

Y	Z	AA	AB
Left Setback Check 1	Right Setback Check 1	Left Setback	Right Setback
211.72	166.39	211.72	166.39
IF(U>(V),V,U)	IF(W>(X),X,W)	IF(Y<0,U,Y)	IF(Z<0,W,Z)

REFERENCES

Allen, P. M., 1972. Urban Geology Along Interstate 35 Growth Corridor From Hillsboro through Ellis County, Texas: Baylor Geological Studies, Bulletin 27.

Allen, P. M., Hayward, O. T., Bernhardt, G., Chintala, R., Flanigan, W., Foster, O., Goforth, T. T., Maier, N. D., McAtee, W., Reed, R., Smith, W., Strube, M., Strohman, W., and Woodruff, C. M., 1993. Anatomy of a Growth Corridor: Geology, Environment, and Engineering Along I-35 Between Dallas and San Antonio: Proceedings of the 36th Annual Meeting of the Association of Engineering Geologists, 311 p.

Allen, P. M. and Narramore, R., 1985. Bedrock Controls on Stream Channel Enlargement with Urbanization, North Central Texas: Water Resources Bulletin, V. 21, No. 6, p. 1037 – 1048.

Ayres Associates, 2004. Erosion Setback Stabilization Criteria for City of Austin Streams: Ayres Project No. 32-0723.00, 80 p.

Baldwin, E. E., 1974. Urban Geology of the Interstate Highway 35 Growth Corridor Between Belton and Hillsboro, Texas: Baylor Geological Studies, Bulletin 27, 39 p.

Bater, C. W. and Coops, N. C., 2008. Evaluating Error Associated with Lidar-derived DEM Interpolation: Computers and Geosciences, doi:10.1016/j.cageo.2008.09.001, 12 p.

Burket, J. M., 1965. Geology of Waco: Baylor Geological Studies, Urban Geology of Greater Waco, Part I: Geology, Bulletin No. 8, p. 9 – 45.

Cameron, T. and Ackerman, P. E., 2005. HEC-GeoRAS: An Extension for Support of HEC-RAS using ArcGIS: U. S. Army Corps of Engineers Hydrologic Engineering Center, OMB No. 0704-0188, 204 p.

Capello, S. V., 2008. Modeling Channel Erosion in Cohesive Streams of the Blackland Prairie, Texas at the Watershed Scale: Baylor University Thesis, 67 p.

Charlton, M. E., Large, A. R. G. and Fuller, I. C., 2002. Application of Airborne LiDAR in River Environments: The River Coquet, Northumberland, UK: Earth Surface Processes and Landforms, V. 28, p. 299-306.

Chin, A., 2006. Urban Transformation of River Landscapes in a Global Context: Geomorphology, V. 79, p. 460 – 487.

Cruden, D. M., Tedder, K. H., and Thomson, S., 1989. Setbacks from the Crests of Slopes along the North Saskatchewan River Valley, Alberta: Canadian Geotechnical Journal, v. 26, p 66 – 74.

City of Dallas, Texas, 1991. Setback from Natural Channel Required. Section 51A-5.106, Ord. No. 21013.

Daly, C. and Taylor, G., 1998. TX_PRECIP_ANNUAL: Water and Climate Center of the Natural Resources Conservation Service. ESRI ArcGIS Shapefile (.shp) Avalilable online at ftp://ftp2.tnris.org/Hydro/Precip/TX_PRECIP_Shp.zip. Accessed 1/27/09.

Daugherty, R. L., Franzini, J. B. and Finnemore, E. J., 1985. Fluid Mechanics with Engineering Applications, McGraw-Hill, Inc., New York, 597 p.

Dempster, G., 1974. Effects of Urbanization on Floods in the Dallas, Texas Metropolitan Area: USGS Water-Resources Investigations 60-73, 51 p.

Doyle, M. W., Huber, J. M., Rich, C. F., and Spacie, A., 2000. Examining the Effects of Urbanization on Streams using Indicators of Geomorphic Stability: Physical Geography, v. 21, no. 2, p 155-181.

The Earth Technology Corperation, 1990. Preliminary Geotechnical Parameters for the Superconducting Super Collider Site: Project No. 87-888-0017, Report No. SSC-GR-69, 69 p.

Elder, W. R., 1965. Soils and Urban Development of Waco, In: Urban Geology of Greater Waco, Part II, Soils: Baylor Geological Studies, Bulletin 9, 66 p.

Font, R. G., and Williamson, E. F., 1970. Geologic Factors Affecting Construction in Waco: Baylor Geological Studies, Urban Geology of Greater Waco, Part IV: Engineering, Bulletin No. 12, 33 p.

Gebert, W. A., Graczyk, D. J. and Krug, W. R., 1987. Average Annual Runoff in the United States, 1951-80: U. S. Geological Survey Hydrologic Investigations Atlas HA-710, Scale 1:7,500,000, 1 Sheet.

Gesch, D. B., 2007. The National Elevation Dataset, In: Maune, D. F. ed., Digital Elevation Model Technologies and Applications: The DEM Users Manual, John Wiley and Sons, New York, p. 99-114.

Harmel, R. D., Richardson, C. W., King, K. W., and Allen, P. M., 2006. Runoff and Soil Loss Relationships for the Texas Blackland Prairies Ecoregion: Journal of Hydrology, V. 331, p 471-483.

Hsu, S. and Nelson, P. P., 2002. Characterization of the Eagle Ford Shale: Engineering Geology, V. 67, p. 169 – 183.

Land, L., Schroeder, E. E., and Hampton, B. B., 1982. Techniques for Estimating the Magnitude and Frequency of Floods in the Dallas-Fort Worth Metropolitan Area, Texas: USGS Water-Resources Investigations 82-18, 62 p.

Leopold, L. B., Wolman, M. G. and Miller, J. P., 1964. Fluvial Processes in Geomorphology, W. H. Freeman and Company, San Francisco, 535 p.

Lo, C. P. and Yeung, A. K.W., 2007. Concepts and Techniques of Geographic Information Systems. 2nd Ed. Upper Saddle River, NJ: Prentice Hall, 544 p.

Manning, R., 1851. Observations on subjects concerned with arterial drainage: Transactions of the Institution of Civil Engineers of Ireland, Part II, IV, 90–104.

Massey, B. C. and Schroeder, E. E., 1977. Application of a Rainfall-Runoff Model in Estimating Flood Peaks for Selected Small Natural Drainage Basins in Texas: USGS Open-file Report 77-792, 23 p.

Meng, X., Wang, L. Silván-Cárdenas, J. S., and Currit, N., 2008. A Multi-directional Ground Filtering Algorithm for Airborne LIDAR: ISPRS Journal of Photogrammetry & Remote Sensing, doi: 10.1016/j.isprsjprs.2008.09.001, 8 p.

Millar, R. G., 2000. Influence of Bank Vegetation on Alluvial Channel Patterns: Water Resources Research, V. 36, No. 4, p. 1109 – 1118.

Narramore, Rebecca, 1981. Stream Channel Enlargement Due to Urbanization in the White Rock Prairie, North Central Texas. Baylor University Thesis, 198 p.

Rayburg, S., Thoms, M. and Neave, M., 2008. A Comparison of Digital Elevation Models Generated from Different Data Sources: Geomorphology, doi:10.1016/j.geomorph.2008.11.007

Robinson, D., 1982. Stream Channel Enlargement due to Urbanization in the Woodbine Formation, Tarrant and Johnson Counties, Texas. Southern Methodist University Thesis, 95 p.

Rosgen, D., 1998. The Reference Reach - a Blueprint for Natural Channel Design: Proceedings of the Wetlands and Restoration Conference, March, 1998, Denver, Co. 9 p.

Rosgen, D.L. (1994). A classification of natural rivers. Catena, V. 22, p. 169-199.

Schueler, T. R., 2000. The Architecture of Urban Stream Buffers: The Practice of Watershed Protection: Article 39, V. 1 No. 4, p. 155-163

Schumm, S. A., 1999. Causes and Controls of Channel Incision, In: Darby, S. E. and Simon, A. eds., Incised River Channels: Processes, Forms, Engineering, and Management, John Wiley and Sons, New York, p. 19-33.

Simon, A. and Hupp, C. R., 1986. Channel Evolution in Modified Tennessee Channels: Proceedings of the Fourth Federal Interagency Sedimentation Conference; March 24-27, 1986, Las Vegas, Nevada, V. 2, p 5.71-5.82.

Soil Survey Staff, Natural Resources Conservation Service, United States Department of Agriculture. Web Soil Survey. Available online at http://websoilsurvey.nrcs.usda.gov/ accessed 1/13/2009.

Texas Parks and Wildlife Department, 1978. Natural_Regions_Maj: Texas Parks and Wildlife. ESRI ArcGIS Shapefile (.shp) Available online at www.tpwd.state.tx.us/nature/tx-eco95.htm . Accessed 2/2/09.

U. S. Geological Survey, 1997. Part 1 General Standards for Digital Elevation Models: National Mapping Program Technical Instructions, 17 p.

United States Department of Agriculture, 2005. National Agriculture Imagery Program, NW Carrolton Quadrangle. Georeferenced Tagged Image File Format (GeoTIFF), available online at ftp://ftp2.tnris.org/Imagery/NAIP04/1m/3296/d329601_1.zip . Accessed 3/2/09.

United States Department of Agriculture, 2005. National Agriculture Imagery Program, SE Garland Quadrangle. Georeferenced Tagged Image File Format (GeoTIFF), available online at ftp://ftp2.tnris.org/Imagery/NAIP04/1m/3296/d329603_4.zip . Accessed 3/2/09.

United States Department of Agriculture, 2005. National Agriculture Imagery Program, SE Lewisville West Quadrangle. Georeferenced Tagged Image File Format (GeoTIFF), available online at ftp://ftp2.tnris.org/Imagery/NAIP04/1m/3397/d339764_4.zip . Accessed 3/2/09.

University of Texas, Bureau of Economic Geology, 1972. Geologic Atlas of Texas, Dallas Sheet: Scale 1:250,000.

Vaze, J. and Teng, J., 2007. High Resolution LiDAR DEM – How Good Is It?: Proceedings of the 2007 Modelling & Simulation Society of Australia & New Zealand Inc., p. 692-698.

Veenhuis, J. E. and Gannett, D. G., 1986. The Effects of Urbanization on Floods in the Austin Metropolitan Area, Texas: USGS Water Resources Investigations Report 86-4069, 66 p.

Ward, A., Mecklenberg, D, Matthews, J. and Farver, D, 2002. Sizing Stream Setbacks to Help Maintain Stream Stability: Proceedings of the 2002 ASAE Annual International Meeting, July 28-31, 2002, Paper No. 022239, 35 p.